Case Studies in Chemical and Environmental Engineering 8 (2023) 100377

Contents lists available at ScienceDirect

Case Studies in Chemical and Environmental Engineering

journal homepage: www.sciencedirect.com/journal/case-studies-in-chemical-and-environmental-engineering

Case Report

Effects of zero-valent iron on sludge and methane production in anaerobic digestion of domestic wastewater

Omari Bakari [a,*], Karoli N. Njau [a], Chicgoua Noubactep [b,c,d]

[a] School of Materials, Energy, Water and Environmental Sciences, Nelson Mandela African Institution of Science and Technology (NM-AIST), Arusha, 23311, Tanzania
[b] Centre for Modern Indian Studies (CeMIS), University of Göttingen, Waldweg 26, D-37073, Göttingen, Germany
[c] School of Earth Science and Engineering, Hohai University, Fo Cheng Xi Road 8, Nanjing, 211100, China
[d] Faculty of Science and Technology, Campus of Banekane, Université des Montagnes, PO Box 208, Bangangté, Cameroon

ARTICLE INFO

Keywords:
Anaerobic digestion
Biogas
Domestic wastewater
Metallic iron
Nutrients
Sludge

ABSTRACT

Iron metal (Fe^0) materials enhance the performance of anaerobic digestion (AD) reactors to remove pollutants. Most research focused on the materials' mechanisms and effectiveness in enhancing AD. However, there is scant information on the biogas and sludge quality and quantity and the kinetics of generated methane (CH_4) of biogas from the Fe^0-aided AD of domestic wastewater (DW). The information is essential for AD reactors' management. This study characterizes the sludge and biogas from Fe^0-aided AD of DW and predicts the CH_4 yield using the Gompertz, Logistic, and Richard models to study the impact of Fe^0 materials on the composition and generation of sludge and biogas. Bench-scale reactors containing DW were fed with Fe^0 and operated for 53 days in a quiescent condition, at 24 ± 3 ^{O}C room temperature, at 7.3 initial pH value. Steel wool and iron scrap were used as Fe^0 sources. A parallel experiment without Fe^0 was performed as an operational reference. Results indicate that Fe^0 significantly enriched most of the nutrients in sludges, produced well-settling sludge (sludge volume index ≤30), and enriched the CH_4 of biogas by more than 12%. Furthermore, all the tested models exhibited good fitting (error <10%) in predicting CH_4 production. Fe^0-aided AD produced a sludge with the potential for application in agricultural land and increased the heating value of the biogas by enriching the CH_4. More than 80% of particles generated from Fe^0-aided AD of DW can be settled in sedimentation tanks designed at an overflow rate ≤40 m/d. Richard was the best model for predicting methane yield from Fe^0-aided AD of DW (error <1.6%).

1. Introduction

Compared to aerobic wastewater treatment systems, anaerobic systems are often practised in developing countries as the appropriate treatment systems because they are affordable, applicable, efficient, and sustainable [1,2]. As opposed to aerobic systems, anaerobic systems facilitate resource recovery from wastes and have relatively low construction, operation and maintenance costs [3–5]. However, further treatment is required for the wastewater effluents from anaerobic reactors to reduce the concentration of residual pollutants, such as organics and nutrients, for compliance [6–8]. Besides other methods such as co-digestion, digester design, and pre-treatment [9–11], additives have been successfully applied in anaerobic digestion (AD) to improve the biodegradability of wastes and the overall pollutants removal efficiency [12]. The additives that are commonly applied include the supplements of iron (Fe), molybdenum (Mo), nickel (Ni), nitrogen (N), phosphorus (P), selenium (Se), sulphur (S), and tungsten (W); compounds such as bentonite, glauconite, phosphorite, zeolites, Fe^0 and Fe^{3+}, and ashes from waste incineration [12]. Fe^0 materials have been recognized as among the effective additives for enhancing the performance of anaerobic digestion reactors due to their abundance, simplicity in manufacturing, low cost, non-toxicity, and environmental friendliness [13–17].

Metallic iron (Fe^0) as additives have been reported in different studies to: (i) enhance anaerobic digestion (AD) systems for various effluents such as domestic wastewater (DW), waste-activated sludge, food wastes, palm oil mill wastewater, swine wastewater, and azo dye wastewater [18–24]; (ii) enhance AD reactors' capacity to remove nitrogen and phosphorus from different wastewaters [25–29]; (iii) increase the performance of individual AD process stages [18,19,30–33];

* Corresponding author.
E-mail addresses: bakario@nm-aist.ac.tz (O. Bakari), karoli.njau@nm-aist.ac.tz (K.N. Njau), cnoubac@gwdg.de (C. Noubactep).

https://doi.org/10.1016/j.cscee.2023.100377
Received 4 April 2023; Received in revised form 5 May 2023; Accepted 15 May 2023
Available online 23 May 2023

(iv) regulate the pH in food wastes AD [20,21]; and (v) increase the percentage composition of methane (CH_4) of biogas from the AD of palm oil mill wastewater, swine wastewater, and activated sludge [19,22,23].

Metallic iron (Fe^0) materials can play a role as a core factor of enzymic activities (e.g. pyruvate-ferrodoxin oxidoreductase) containing Fe–S clusters and facilitate fermentation in the hydrolysis stage [34]. Moreover, the materials can simultaneously relieve the suppression of un-dissociated hydrogen sulphide (H_2S) on various microorganisms, including acetogenic, methanogenic and sulfate-reducing bacteria (SRB) [35,36]. The inhibition relief is achieved through pH buffering (Equation (1)) and precipitation of iron sulphide (Equation (2)) [36,37]. Besides, propionic fermentation occur at oxidation-reduction potential (ORP) above −278 mV [31,38]. In lower ORP, propionic shifts to acetic fermentation and favours CH_4 production [39]. The dosage of Fe^0 to the reactor for acidogenesis reaction simultaneously dropped the accumulation of propionate from 416 to 225 mg/L and raised the acetate production from 222 to 408 mg/L [31]. These results were linked to the inherent capacity of Fe^0 to lower ORP [30,31]. Moreover, hydrogen (H_2) that is normally released during the corrosion of Fe^0 donates electrons to various H_2-respiring microbes, including methanogens (equation (3)) and denitrifying bacteria (Equation (4)) [40,41]. The inclusion of Fe^0 in wastewater treatment has been communicated to enhance bacterial growth to realize biological wastewater treatment [42].

$$Fe^0 + 2H_2O \rightarrow Fe^{2+} + H_2 + 2OH^- \tag{1}$$

$$8H^+ + 4Fe^0 + SO_4^{2-} \rightarrow S^{2-} + 4Fe^{2+} + 4H_2O \tag{2}$$

$$CO_2 + 4H_2 \rightarrow CH_4 + 2H_2O \tag{3}$$

$$2NO_3^- + 5H_2 \rightarrow N_2 + 4H_2O + 2OH^- \tag{4}$$

Most studies on integrating Fe^0 materials in AD reactors focused on the potential to improve the reactors' capability to remove different organic and inorganic pollutants. The pollutants include carbon (C), nitrogen (N), sulphur (S), phosphorus (P), heavy metals, chlorinated organic compounds, nitroaromatic compounds, dyes, and others from polluted waters or sludges as documented in different review papers [16,28,43–51]. Nevertheless, the information about the effect of Fe^0 on the quantity and quality of biogas and sludge produced from Fe^0-aided AD of DW that could be used for management purposes is scant. Furthermore, there is also scant information on the kinetic modelling of CH_4 generated from Fe^0-aided AD of DW. The kinetic modelling of CH_4 production is an acceptable method for determining specific operational parameters of AD systems [52]. The parameters include cumulative specific CH_4 production, maximum specific CH_4 production potential, specific rate of CH_4 production, and phase delay time [53–55].

Each Fe^0 material (e.g., IS or SW) has its intrinsic reactivity [56–58]. Adding more reactive Fe^0 materials or a more significant amount of less reactive ones to aqueous systems forms more precipitates of Fe^0 corrosion products (FeCPs) [56,59,60]. The FeCPs enmesh and adsorb pollutants while settling down [60–62] to form more sludge with elevated concentrations of such pollutants. The sludge, for instance, may contain macro-nutrients (calcium (Ca), magnesium (Mg), nitrogen (N), phosphorus (P), potassium (K) and sulphur (S)), micro-nutrients (copper (Cu), iron (Fe), manganese (Mn) and zinc (Zn)), carbon (C) and toxic elements such as chromium (Cr), nickel (Ni) and lead (Pb) in concentrations acceptable or above the ceiling limits for application in agricultural land [5,63,64]. On the other hand, precipitation of S as Fe_2S [65–70] and N as ($FeNH_4PO_4.H_20$) [71–73], for instance, may reduce the concentration of H_2S and ammonia (NH_3) gaseous impurities of the produced biogas. The higher the CH_4 content (with fewer impurities, e.g., H_2S and NH_3) in biogas, the higher the biogas' potential for energy recovery [4,74]. Although the energy content of biogas depends mainly on its CH_4 gas content, the gas needs to be controlled (not released to the atmosphere) as it is more potent (about 21 folds) than carbon dioxide (CO_2) for inducing the greenhouse effect [74,75]. The current study focused on the characterization of solids and biogas generated in Fe^0-aided AD of DW. The study also evaluated the Logistic, modified Gompertz, and Richard models for assessing the kinetic of CH_4 production. To our knowledge, the evaluation of models for predicting CH_4 yield from Fe^0-aided AD of DS has not been done. Different quantities of biogas and sludge from the tested Fe^0-aided AD reactors were expected in this study on account of different; (i) Fe^0 materials types (Iron Scrap (IS) and Steel Wool (SW)) and (ii) amounts (dosages) of IS materials (0 g/L and 10 g/L). This study applied IS and SW materials as sources for Fe^0 since they are easily obtainable, inexpensive and have good reactivities founded on the experimental results of previous studies [56,76]. Similarly, the 10 mg/L dosages of Fe^0 (IS and SW) were used in this study because our previous study [59] with the same materials found that 10 mg/L was the optimum dose for removing of organics and nutrients from DW.

Biogas and sludge samples from the tested Fe^0-aided anaerobic batch reactors (10 g/L IS or 10 g/L SW) and the reference reactor (reactor without Fe^0) were analyzed to compare the reactors' significances in enriching the generated; (i) sludge with organics, nutrients and toxic elements and (ii) biogas with CH_4 or other gaseous impurities such as H_2S, CO_2, and NH_3. The basis for comparison was; (i) the difference in concentrations of the organics, nutrients and toxic elements in the sludge between the anaerobic reactors with Fe^0 materials (10 g/L IS or 10 g/L SW) and the reference (0 g Fe^0/L) (ii) difference in concentrations of CH_4, H_2S, CO_2, and NH_3 between the reactors dosed with Fe^0 (10 g/L IS or 10 g/L SW) and the reference (0 g Fe^0/L). The 10 g Fe^0/L dosage selection was based on our previous lab-scale optimization studies [59] with the same materials in removing organics and nutrients from DW. However, different optimum dosages ($\leq$30 g Fe^0/L) of different types of Fe^0 material with various wastes have been reported [20,23,77–79]. This research studied the significance of Fe^0-aided AD of DW to enrich (i) nutrients in sludge and (ii) CH_4 in biogas reactors for managing such reactors.

2. Materials and methods

2.1. Materials

2.1.1. Inoculum sludge and wastewater

Table 1 presents the quality of the inoculum sludge and tested domestic wastewater. The sludge and domestic wastewater were sampled from the septic tank at the Nelson Mandela African Institution of Science and Technology (NM-AIST). The septic tank is dedicated to treating wastewater from the students' hostels. In order to avoid floating objects, oil, and grease as much as possible, the wastewater sample was collected below the scum.

2.1.2. Fe^0 materials

Iron Scrap (IS)and commercial steel wool (SW) were the Fe^0 materials used in this study. The IS materials were the waste products from the lathing machine. The tested SW (Africa Limited) was a commercial product bought on the local market in Tengeru (Tanzania). The SW was slashed into lengths of about 20 mm, while IS sizes ranged from 4 mm to 20 mm (Fig. 1). The steel wool materials used had an iron content of 99.25%, while the scrap iron materials had 98.68% (Table 2). Furthermore, the dissolution rates were 4.41 μg/h for IS and 5.05 μg/h for SW [59]. The Fe^0 materials used in this study are the same as the Fe^0 materials used in our previous study [59], where detailed information about the characteristics and reactivity of the materials is reported.

2.2. Experimental procedure

2.2.1. Characteristics of sludge and biogas

An experiment was designed to anaerobically digest the DW dosed with Fe^0 materials in a monitored environment to obtain and then

Table 1
Essential quality of inoculum sludge and tested domestic wastewater.

Parameters	M (n = 3)	SD (n = 3)
I – Quality of Dry Inoculum sludge		
Potential of hydrogen, pH (1:2.5)	6.83	0.02
Chemical oxygen demand, COD (gCOD/L)	3.945	0.004
Total solids, TS (gTS/L)	14.75	0.04
Total volatile solids, TVS (gVS/L)	7.98	0.1
Volatile Suspended solids, VSS (gVSS/L)	5.57	0.2
Total Organic Carbon, TOC (%)	27.1	1.1
Total Kjeldahl Nitrogen – TN (%)	0.81	0.03
Sulphur, S (mg/kg)	0.51	0.03
Extractable Phosphorus – P (mg/kg)	135.7	3.4
Potassium, K (%)	0.02	0.003
Magnesium, Mg (%)	7.2	0.4
Calcium, Ca (%)	4.83	0.3
Iron, Fe (%)	0.11	0.03
Manganese, Mn (mg/kg)	285.2	4.9
Copper, Cu (mg/kg)	9.9	0.7
Zinc, Zn (mg/kg)	306.2	6.2
Chromium, Cr (mg/kg)	23.7	1.3
Nickel, Ni (mg/kg)	5.8	0.6
Lead, Pb (mg/kg)	0.34	0.04
II – Quality of tested domestic wastewater		
Potential of hydrogen, pH	7.51	0.03
Temperature, T (^oC)	22	0.1
Chemical oxygen demand, COD (gCOD/L)	428	3.6
Orthophosphate, PO_4^{3-} (mg PO_4^{3-}/L)	28.6	0.6
Nitrate, NO_3^- (mg NO_3^-/L)	24.8	0.9
Ammonium, NH_4^+ (mg NH_4^+/L)	55.5	1.5
Sulfate, SO_4^{2-} (mg SO_4^{2-}/L)	41.4	1.2

''M'' stands for mean, and ''SD″ for standard deviation.

characterize the resulting biogas and sludge. The experimental set-up involved bench-scale plastic anaerobic reactors, each with 60 L capacity (Fig. 2(a)). The first reactor (Reactor I) was used as a reference (Table 3). Except for the reference reactor, which was fed with 50 L of DW and 3 L of inoculum only, each of the other two reactors (Reactors II and III) was fed with 50 L of DW, 3 L of inoculum and 10 g/L of Fe^0 materials (Table 3). The COD/VS (Wastewater/Inoculum) was 5.4%. Reactor II was fed with IS, while Reactor III was with SW materials (Table 3) to compare the effect of dissimilar Fe^0 materials on biogas and sludge quantity and quality. The same inoculum and DW were used in each tested reactor. The 10 g/L dosages of Fe^0 material were adopted because our previous lab-scale study [59] with the same materials established the dose as optimum for organics and nutrient removal. All the anaerobic reactors were operated parallelly for 53 days at quiescent conditions, batch mode, room temperature of 24 ± 3 ^OC, and initial pH of 7.3. The biogas monitoring was also done for 53 days of reactors' operation because, after that period, the amount of biogas generated was too small to measure.

$$Fe^0 \text{ to inoculum ratio } \left(g\ Fe^0 / g\ TS\right) = \frac{Fe^0 \text{ dosage } \left(g/_L\right)}{\text{TS of the inoculum sludge } \left(g/_L\right)}$$

Where; Fe^0 dosage = 10 g/L for IS or SW (Table 3), and TS of the sludge = 14.75 g/L (Table 1).

Treated DW samples (50 mL) were collected from each reactor twice a week for COD and pH analysis. The biogas samples from the airbag were collected and analyzed daily for the first two weeks of the reactor's operation. The subsequent sampling and analysis were done after collecting at least 300 ml of biogas from the slowest biogas-releasing reactor. The analysis of the generated biogas was for determining the volume and composition. A portion of the sludge sample from each bench-scale reactor was drawn through the sludge sampling port (Fig. 2 (a)) and analyzed for TS, TSS, VSS, and settleable solids at the end of the 53 days of the experiment. Another portion of the sludge samples was air dried (in the absence of direct sun rays) and analyzed for macro-nutrients (Ca, K, Mg, N, P, and S), micro-nutrients (Cu, Fe, Mn, and Zn), organic carbon, pH, and toxic elements (Cr, Ni, and Pb). All the experiments were performed in triplicates.

2.2.2. Settling experiment

The settling test of solids resulting from 53 days of anaerobically digested DW in each bench-scale reactor (Fig. 2(a)) was done in a settling column (Fig. 2(b)). The analysis aimed to determine the solids settling velocities and overall TSS removal efficiencies at 90 min and 120 min settling times for the samples collected from the port at 2.5 m column depth for comparison purposes. The settling column was fabricated using a class C uPVC pipe with a nominal outside diameter of 160mm. The column was 3 m tall with an effective side water depth of 2.5 m. The sampling ports were provided at an equal interval of 500 mm from the top (Fig. 2(b)). The content from each reactor was manually

Table 2
Elemental composition of tested Fe^0 materials. LOD stands for the lowest concentration at which an element can be detected.

Name	Elemental composition (%)							
	Fe	Cu	Ni	Cr	Mn	Sn	Nb	Mo
Steel wool (SW)	99.25	0.09	0.09	0.04	0.50	< LOD	< LOD	< LOD
Steel scraps (IS)	98.68	0.33	0.15	0.27	0.40	0.07	0.01	0.02

(a)　　　(b)

Fig. 1. Size specification of Fe^0 materials tested – (a) Scrap iron (b) Steel wool.

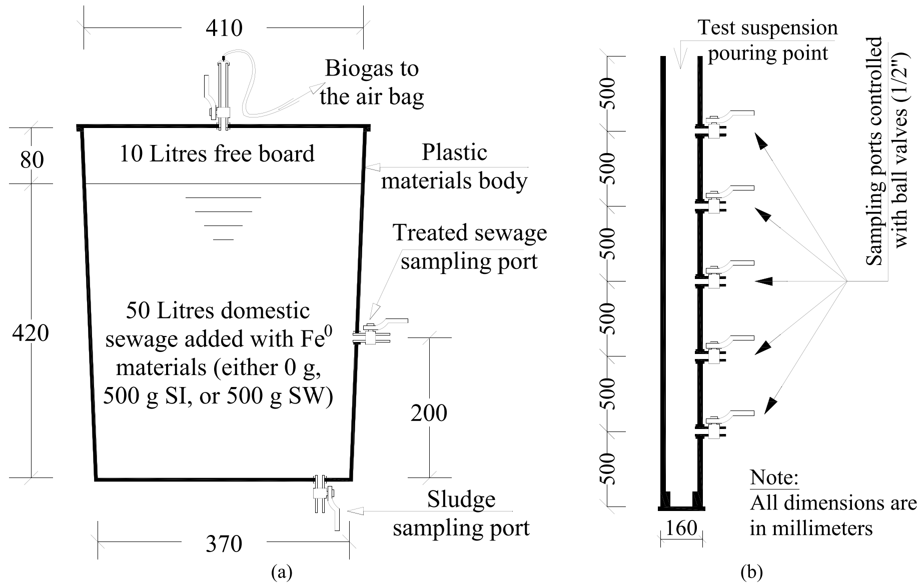

Fig. 2. Experimental set-up (a) Anaerobic digester with 60 L capacity (b) Settling column.

Table 3
Identities of reactors used in the bench-scale study.

Reactor	Medium	Fe^0 material	Fe^0 dosage (g/L)	Fe^0 to inoculum ratio (g Fe^0/g TS)
I	DW	none	0	0.0
II	DW	IS	10	0.7
III	DW	SW	10	0.7

"DW" stands for Domestic Wastewater, "IS" for Iron Scrap, "SW" for steel wool and TS for total solid. The Fe^0 materials dosages measurement accuracy was 0.1 g Fe^0/L.

stirred to obtain a uniform suspension of particles before quickly taking a sample to measure the initial TSS concentration and pouring the content into the settling column through the top. The stirring was done for an average of 10 seconds by inverting the capped container five (5) times. The amount of sludge involved in each settling column test was 3 L. The samples were drawn simultaneously from all ports of the settling column every 10 minutes for 150 minutes. The collected samples were then analyzed for TSS in triplicate. The method for column settling analysis is well described in various literature [3,5,80–83].

2.3. Analytical methods

The names of methods used for the analyzed parameters were: aqua regia for K, Mg, Ca, Na, S, Fe, Mn, Cu, Zn, Cr, Ni, and Pb; Olsen for P; Kjeldahl for TN; and Walkley-black for organic carbon; Low Range (LR) reactor digestion for COD; Nessler reagent for NH_4^+, High Range (HR) Cadmium reduction for NO_3^-, PhosVer 3 for PO_4^{3-}. The pH of sludge was measured in 1:2.5 sludge: water using an Accsen benchtop pH meter by Lasec SA (Pty) Ltd, while that of DW was measured using an Orion star A214 pH meter. The K, Mg, Ca, and Na were measured using a Flame photometer (Model 2655–00) manufactured by Cole-Parmer Company based in Chicago, USA. On the other hand, Fe, Mn, Cu, Zn, Cr, Ni, S, and Pb were measured using Thermo scientific iCE 3000 series atomic absorption spectrometer designed in the UK; P using Spectronic 200E UV-VIS spectrometer by Thermo Fisher Scientific based in China. TKN by Kjeldahl distillation unit manufactured by Jinan Biobase Biotech Co. Ltd based in China. Parameters such as COD, NH_4^+, NO_3^-, and PO_4^{3-} were measured using a spectrophotometer (DR2800), the product of HACH Company. The syringe method was used to measure the generated biogas volume, while the composition analysis was done with a biogas analyzer (Geotech biogas 5000 analyzers).

2.4. Statistical data analysis

Graph plotting was accomplished using either Microsoft Excel 2019 or AUTOCAD 2018 soft. The AUTOCAD 2018 was used only in plotting the percent removal and Isoremoval curves for settling column analysis. The statistical analysis of the gathered data was performed using Microsoft Excel 2019. The Microsoft Excel software was used to determine the statistical significance tests for $n < 30$ observations ions, two-tailed student t-test, degrees of freedom of $n - 2$, and $p = 0.05$ confidence interval. The *t*-tests were performed to assess whether there was a significant difference in the observed nutrients and organic matters concentrations in the produced sludge and biogas quantity and quality between (i) the reference reactor and the reactors with Fe^0 materials and (ii) the reactor with IS materials and that with SW materials.

2.5. Determination of overall TSS removal efficiency

The AUTOCAD program was used only in plotting per cent removal and isoremoval curves graphs, while the Excel program was used in plotting all other graphs and calculations. The per cent TSS removal values were calculated using equation (5) and plotted as points in circles against time and depth (Fig. 3 (a), (b) and (c)). Settling velocity (overflow rate) and the overall TSS removal efficiency achieved in the settling analysis of particles generated by each reactor was calculated using curves shown in Fig. 3, together with the formula presented in equations (6) and (7).

$$\eta = \left(\frac{C_0 - C_{ti}}{C_0}\right) \times 100 \tag{5}$$

Where; η = TSS removal efficiency (%), C_0 = Initial TSS concentration (mg/L), and C_{ti} = TSS concentration observed at time t for *i*th port (mg/L).

$$V_s = \frac{H}{t_s} \tag{6}$$

Where; V_s = Settling velocity (m/min), H = side water depth that is equal to or less than settling column height (m), and t_s = time required to achieve a particular percentage removal of particles in the settling column analysis (min).

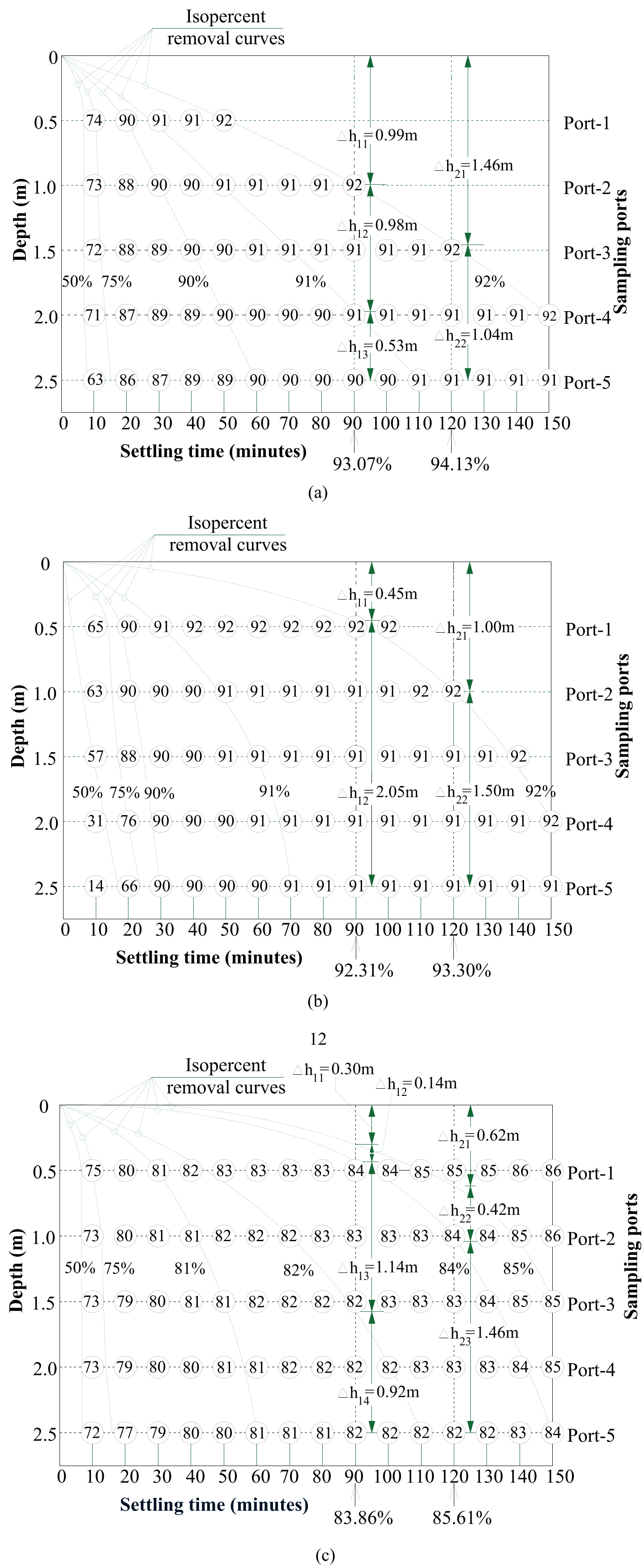

Fig. 3. Percent removal and Isoremoval curves for settling column analysis (a) Reactor without Fe^0 materials (b) Reactor dosed with 10 mg/L IS materials (c) Reactor dosed with 10 mg/L SW materials.

$$R_T = \frac{\Delta h_1}{H}\left(\frac{100+R_1}{2}\right) + \frac{\Delta h_2}{H}\left(\frac{R_1+R_2}{2}\right) + \ldots\ldots + \frac{\Delta h_n}{H}\left(\frac{R_n+R_{n+1}}{2}\right) \quad (7)$$

Where; R_T = Overall TSS removal, (%), $\Delta h_1, \Delta h_2, \ldots, \Delta h_n$ = vertical distance between two consecutive curves of equal percent removal, (m), $R_1, R_2, \ldots, R_n$ = consecutive isoremoval curves, (%).

2.6. *Kinematic models for methane production*

Different models have been applied to determine the kinetics of CH_4 generation [53–55]. The models are used to predict the cumulative CH_4 yield, estimate CH_4 generation potential, determine the daily maximum CH_4 generation and establish the lag phase required to start CH_4 production [84]. However, in this study, the kinetics of CH_4 generation from Fe^0-aided AD of DW was evaluated using the modified Gompertz (equation (8)), Logistic (equation (9)) and Richard (equation (10)) models. Gompertz, Logistic and Richard are among the most appropriate models for CH_4 generation prediction [85]. Regression analysis was done in Excel using the data analysis toolpak add-in to evaluate the models predicting CH_4 production at a 95% confidence interval. The average observed cumulative CH_4 production was used to evaluate the models.

$$y = A.exp\left[-exp\left(\frac{\mu_m.e}{A}.(\lambda - t) + 1\right)\right] \quad (8)$$

$$y = \frac{A}{\left[1 + exp\left(\frac{4\mu_m}{A}.(\lambda - t) + 2\right)\right]} \quad (9)$$

$$y = A.\left\{1 + v.exp(1+v).exp\left[\frac{\mu_m}{A}.(1+v).\left(1+\frac{1}{v}\right).(\lambda - t)\right]\right\}^{\left(\frac{1}{v}\right)} \quad (10)$$

Where: y = cumulative specific CH_4 production (mLCH_4/gVS); A = maximum specific CH_4 production potential (mLCH_4/gVS); μ_m = specific rate of CH_4 production (mL/gVS/d); $e = \exp(1) = 2.7182$; λ = phase delay time (days); t = incubation time (days); and v = shape coefficient of the curve.

3. Results and discussion

3.1. *Effects of Fe^0 materials types on sludge quantity and quality*

3.1.1. *Physical characteristics of sludge*

Results of solids analysis of the sludges produced from different dosages of materials in anaerobic reactors are presented in Tables 4 and 5. The results in Table 4 indicate that compared to the reference reactor, the Fe^0 – aided anaerobic reactors produced sludge with more weight, volume, TSS, and VSS. For instance, 10 g/L IS reactor produced 275 mL/L of sludge (settled sludge), more than 1.4 times the 190 mL/L produced in the reference reactor. However, the reference produced sludge with VSS to TSS ratio of 69%, which is the highest compared to 52% for 10 g/L IS reactor and 45% for 10 g/L SW reactor.

A higher volume of sludge generated from Fe^0-aided anaerobic reactors compared to the reference system may be linked to (i) accumulation of passivated Fe^0 solids [23], (ii) higher biomass generation due to the proliferation of microbial population enhanced by Fe^0 materials [24,25], and (iii) solids from enhanced precipitation and adsorption of pollutants by FeCPs [56,59,60]. Results in Table 5 indicate that the observed TSS concentration at 60 min, 90 min, and 150 min settling times were 329 mg/L, 319 mg/L and 310 mg/L for 10 g/L IS reactor and 663 mg/L, 635 mg/L and 555 mg/L for 10 g/L SW reactor respectively. The results suggest that relatively more solids will remain suspended (unsettled), and hence lower sludge will be collected in 10 g/L SW than in 10 g/L IS reactor. Because steel wool (SW) materials are more reactive than IS [59,76], it is perceived that SW materials were highly corroded to form a more concentrated (Table 5) range of finer particles with less settling velocities compared to the particles from Iron Scrap (IS) materials.

On the other hand, the overall solid removal efficiencies achieved at the settling times of 60 min and 90 min were 93.07% and 94.13% for the reference reactor, 92.31% and 93.30% for 10 mg/L IS reactor and 83.86% and 85.22% for 10 mg/L SW reactor (Fig. 3 (a), (b) and (c)). The 90 min and 120 min settling times at 2.5 m column depth correspond to settling velocities (overflow rates) of 40 m/day and 30 m/day.

The results suggest the possibility of removing more than 80% of particles generated from Fe^0-aided AD of DW using sedimentation tanks (clarifiers) designed at an overflow rate of 40 m/d or below. Moreover, the results indicate that the Fe^0– aided AD generates more suspended solids with lower average settling velocities than anaerobic digesters without such materials. Apart from normal biosolids generated from the AD of solids from DW, some particles result from precipitation and the adsorption of pollutants by the Fe^0 materials FeCPs. The low settling velocity may be due to the different nature and sizes of precipitates from Fe^0– aided anaerobic reactors. For instance, nitrogen may be removed as metal ammonium phosphates ($FeNH_4PO_4.H_20$) [71–73]; phosphates as ferric phosphates precipitates ($Fe_{0.8}HPO_4(OH)_{1.4}$) and; sulphur as iron sulphide (Fe_2S) [5,65–68,86,87]. Although the average settling velocity of the solids from the reactors dosed with Fe^0 materials is perceivably lower than that of the solids from the reference (Fig. 3), the fraction of solids with relatively higher settling velocities was enough to form more sludge in the reactors dosed with Fe^0 materials than in the reference reactor (Table 4). Adding Fe^0 materials has been reported to increase the size and settling rate of granules formed in municipal wastewater treatment [88]. However, the sludges from all reactors are generally classified as well-settling because their SVIs are less than 100 (Table 4) [3,83,89–91].

Table 4
Comparison of the physical characteristics of sludges from different reactors.

Sample parameters	Unit	Systems					
		0 g/L		10 g/L SI		10 g/L SW	
		M	SD	M	SD	M	SD
Sludge weight at 105 °C (TS)	kg/m^3	9.2	0.38	15.5	0.41	20.5	0.43
TSS	mg/L	8730	7.8	14550	8.1	19520	8.6
VSS	mg/L	6040	6.2	7550	7.1	8720	7.8
VSS/TSS	%	69	1.3	52	1.5	45	1.7
Sludge volume/ Settleable solids (After 30 min settling time)	mL/L	190	2.4	275	2.2	200	2.3
Sludge volume index (SVI)	mL/gTSS	22	0.7	19	0.5	10	0.8

"TS" stands for total solids, "VSS" for volatile suspended solids, "TSS" for total suspended solids, "M" for mean, and "SD" for standard deviation.

3.1.2. *Chemical characteristics of sludge*

3.1.2.1. Organic matters. The organic matters concentrations in the

Table 5
TSS concentrations for domestic wastewater from different reactors as observed at 2.5 m depth of the settling column.

Reactor name	TSS_o (mg/L)		TSS_{60} (mg/L)		TSS_{90} (mg/L)		TSS_{150} (mg/L)	
	M	SD	M	SD	M	SD	M	SD
0 g/L	2510	8.4	257	7.4	244	6.6	217	5.8
10 g/L IS	3433	10.1	329	9.8	319	9.1	310	8.7
10 g/L SW	3506	12.2	663	10.8	635	11	555	9.7

"M" stands for mean, "SD" for standard deviation, and "TSS_0″, "TSS_{60}″, and "TSS_{150}″ for total suspended solids concentrations at 0 min, 60 min, and 90 min settling times, respectively.

three different types of sludges tested are presented in Table 6. The results indicate that there were relatively higher N and S but lower organic carbon concentrations in the sludge from the reactors dosed with Fe^0 materials than in the reference reactor (Table 6). Results for the tested sludges from the tested anaerobic reactors (I, II, and III) indicate that statistically: (i) there was a significant difference in the observed concentrations of organic matters (C, N, and S) and C/N ratio between reactor I and II or III, $p < 0.05$, two-tailed (Table 6) (ii) there was a significant difference in the observed concentrations of C and N, and C/N ratio between Reactor II and III, $p < 0.05$, two-tailed (Table 6) (iii) there was no significant difference in the observed S concentrations between Reactor II and III, $p < 0.05$, two-tailed.

The relatively lower amount of organic carbon in the sludges from reactors II and III (Table 6) is perceivably due to the higher conversion of organics to CO_2 and CH_4 [40,66,92,93]. The COD removal and biogas production is higher in the Fe^0-aided anaerobic reactors compared to the reactor without Fe^0 materials, as shown in section 3.2 and elsewhere [23,59,94–99]. Moreover, adding Fe^0 materials leads to the accumulation of passivated Fe^0 solids [23,59,100] that contribute to the increase in the inorganic solids in the Fe^0-aided anaerobic reactors compared to the reactor without Fe^0 (reference). On the other hand, a relatively higher amount of N in Fe^0 materials dosed reactors compared to the reference reactor may be due to the precipitation of nitrogen as metal ammonium phosphates ($FeNH_4PO_4.H_20$) [71–73] and nitrogen released from the dead microbes. Fe0-aided AD is associated with the proliferation of microbial populations [24,25]. Furthermore, a higher amount of S in Fe^0 materials dosed reactors than the reference may be due to the precipitation of iron-sulphide (FeS) due to Fe^0 materials dosage [65–68, 86].

On the other hand, the relatively higher concentration of organic matter (C, N, and S) in the sludges from reactor II compared to that from reactor III is perceivably due to a higher accumulated amount of FeCPs in reactor III compared to reactor II. Because SW materials are more reactive than IS materials [29,56,59,101], more FeCPs may have contributed to the increase in the percentage of inorganic solids in reactor III than II.

The mass C/N ratio of the sludges from the reactors was 34 for 0 g/L, 9 for 10 g/L IS and 5 for 10 g/L SW (Table 6). The C/N ratio in the reactors dosed with Fe^0 materials were below the optimum range of 25–35 for the composting process [102]. The relatively higher N and lower C contents in the sludges from the systems dosed with Fe^0 materials resulted in lower C/N ratios than the control system (Table 6). Therefore, during AD of the sludge from Fe-aided anaerobic digestors, materials with more organic carbon, such as sawdust, rice husks, leaves, wood chips, and old compost, may be added to regulate the C/N ratio [102]. However, the results clearly show that the Fe^0 -aided AD increased the concentration of N and S by more than 1.5 times that of the N and S in the reference reactor (Table 6). Therefore, the sludge from the Fe^0 - aided anaerobic reactors can potentially increase soil organic matter for N and S if applied to land.

Table 6
Comparison of the observed parameters' concentrations in dry sludges from the tested anaerobic digestion reactors.

Groups	Parameters	Reactor I		Reactor II		Reactor III	
		M	SD	M	SD	M	SD
Micronutrients and toxic elements to plants	Fe (%)	0.1	0.01	7.6	0.4	14.6	0.8
	Mn (mg/kg)	270.9	2.3	584.5	2.9	948.4	3.2
	Cu (mg/kg)	9.5	0.5	249.8	1.5	420	2.2
	Zn (mg/kg)	298.2	1.9	534.8	3.3	376	2.0
	Cr (mg/kg)	22.0	0.5	25.4	1.0	27.2	1.0
	Ni (mg/kg)	6.0	0.4	45.6	0.8	58.0	1.1
	Pb (mg/kg)	0.25	0.04	1.4	0.1	3.1	0.1
	Cd (mg/kg)	ND	-	ND	-	ND	-
Macronutrients	P (mg/kg)	129.2	3.6	280.4	4.3	364.2	4.9
	K (%)	0.02	0.003	0.07	0.002	0.08	0.003
	Mg (%)	6.29	0.53	0.2	0.02	0.51	0.03
	Ca (%)	4.67	0.25	3.5	0.17	1.33	0.06
	SAR	0.1	0.02	0.8	0.13	2.3	0.2
Organic matters	N (%)	0.78	0.03	1.78	0.07	1.48	0.06
	S (mg/kg)	0.42	0.05	0.94	0.07	0.82	0.06
	C (%)	27.1	1.3	15.8	0.9	6.6	0.8
	C/N	34	0.3	9	0.8	5	0.6
	pH (1:2.5)	6.16	0.01	6.57	0.02	6.96	0.02

"M" stands for mean and "SD" for a standard deviation for $n = 3$; ND for not detected.

3.1.2.2. Macro-nutrients. The concentrations of macro-nutrients in the three different types of sludges tested are presented in Table 6. The results indicate relatively higher N, P, K, S and SAR but lower mg and Ca concentrations in the sludge from the reactors dosed with Fe^0 materials than in the reference reactor (Table 6). The sludges analysis results for the tested Fe^0-aided anaerobic reactors (0 g/L, 10 g/L IS, and 10 g/L SW) indicate that statistically: (i) there was a significant difference in the observed concentrations of macro-nutrients (N, P, K, Mg, Ca, and S) and SAR between reactor I and II, $p < 0.05$, two-tailed or reactor III, $p < 0.05$, two-tailed (Table 6) (ii) there were significant differences in the observed concentrations of macro-nutrients (N, P, Mg, Ca, and S) and SAR between reactor II and III, $p < 0.05$, two-tailed (Table 6) (iii) there was no significant difference in the observed K concentrations between reactor II and III, $p > 0.05$, two-tailed (Table 6).

The relatively higher concentrations of parameters such as N, P, K, and S in the sludge from Fe^0 materials dosed reactors compared to the reference reactor may be due to the following reasons; (i) precipitation of N and P as metal ammonium phosphates [73] (ii) precipitation of S as Fe_2S [65–68,86,87] (iii) possibility of precipitation of K as $FeKPO_4$ [103]. Although precipitation of P with Fe reduces the availability of P due to the strength of their bond [86], the results in Table 6 indicate that extractable P has increased by more than two times in the reactors dosed with Fe materials compared to the reference reactor (reactor without Fe^0 materials). For that reason, more P could be recovered perceivably if the sludges were further treated with lime or other known P recovery methods [104,105]. On the other hand, relatively lower concentrations of Ca and Mg metals in the sludge from reactors dosed with Fe^0 materials are perceivably due to; (i) the dominance of iron in the reactors that make it the favourable cations for precipitation of available anions and (ii) higher affinity of iron to anions such as phosphorus and therefore may cause less precipitation of compounds such as calcium phosphate ($Ca_3(PO_4)_2$) and struvite ($MgNH_4PO_4$) [69].

3.1.2.3. Micronutrients and toxic elements to plants. Results on the observed concentration of the micronutrients (Fe, Mn, Cu, and Zn) and toxic elements (Cr, Ni and Pb) in the three different types of sludges are presented in Table 6. Concentrations of micronutrients in the sludge from the reactor without Fe^0 materials were lower than those dosed with Fe^0 materials. Therefore, it is perceived that Fe^0-aided AD of DW has the potential to concentrate micronutrients and toxic elements in the sludge.

The sludges analysis results for the tested Fe^0-aided anaerobic reactors (0 g/L, 10 g/L IS, and 10 g/L SW) indicate that statistically, there was: (i) significant difference in the observed concentrations of micronutrients (Fe, Mn, Cu, and Zn) and toxic elements (Cr, Ni, and Pb) between Reactor I and II, $p < 0.05$, two-tailed or Reactor III, $p < 0.05$, two-tailed (Table 6) (ii) significant difference in the observed concentrations of micro-nutrients (Fe, Mn, Cu, and Zn) and toxic elements (Ni and Pb) between Reactor II and III, $p < 0.05$, two-tailed (Table 6) (ii) no significant difference in the observed Cr concentrations between Reactor II and III, $p > 0.05$, two-tailed (Table 6).

The relatively higher concentrations of metals such as Mn, Cu, Zn, Cr, Ni and Pb in the sludge from Fe^0 materials dosed reactors compared to the reference reactor is perhaps due to adsorption onto the surface of metallic iron materials or FeCPs [106]. Furthermore, being more reactive (hence producing more FeCPs) than Iron Scrap materials [59], maybe the reason for the relatively higher concentration of micro-nutrients and toxic elements in reactor III compared to II (Table 6).

However, the concentration of toxic elements in the sludges from the reactors (II and III) dosed with Fe^0 materials (Table 6) are far better than the European Directive 86/278/EEC proposed allowable concentrations of heavy metals in Wastewater sludge used in agriculture: 20 to 40 for Cd, 1000–1750 mg/kg for Cu, 300–400 mg/kg for Ni, 750–1200 mg/kg for Pb, 2500–4000 mg/kg for Zn, and Cr is not limited [64]. Similarly, the concentrations are also far better than US EPA pollutant ceiling concentrations (85 mg/kg for Cd, 3000 mg/kg for Cr, 4300 mg/kg for Cu, 840 mg/kg for Pb, 420 mg/kg for Ni, and 7500 mg/kg for Zn) for the land application of Wastewater sludge [63]. Therefore, sludges from Fe^0-aided AD of DW contain heavy metals within acceptable concentrations for application in agricultural lands.

3.2. *Effects of Fe^0 materials types on biogas quantity and quality*

Fig. 4 compares the effects of Fe^0 types on the quantity and quality of the produced biogas. Results indicate that the maximum CH_4 contents (Fig. 4 (a)) and cumulative specific CH_4 yield (Fig. 4(e)) achieved in the tested reactors were 79.8% and 684.3 mLCH_4/gVS for 10 g/L IS, 78.9% and 609.8 mLCH_4/gVS for 10 g/L SW and 67.4% and 422.6 mLCH_4/gVS for the reference reactor. Based on the cumulative specific CH_4 yield (Fig. 4 (e)), adding 10 g/L IS increased CH_4 gas production by 38.3%, while adding 10 g/L SW increased the gas production by 30.7%. On the other hand, the maximum observed concentration of CO_2 (Fig. 4 (b)), H_2S (Fig. 4 (c)), and NH_3 (Fig. 4 (d)) were 7.9%, 135 ppm and 97 ppm for 0 g/L, 6.7%, 93 ppm and 68 ppm for 10 g/L IS, and 7.0%, 70 ppm and 62 ppm for 10 g/L SW.

Moreover, the results presented in Fig. 4(f) indicate that specific CH_4 yields were 0.22 m^3/kgCOD for reactor I (0 g/L), 0.33 m^3/kgCOD for reactor II (10 g/L IS), and 0.31 m^3/kgCOD for reactor III (10 g/L SW). Generally, the results indicate that: (i) reactors with Fe^0 materials (IS or SW) produced biogas with higher CH_4 (Fig. 4 (a)) but lower CO_2 (Fig. 4 (b)), H_2S (Fig. 4 (c)), and NH_3 (Fig. 4 (d)) contents compared with the reactor without Fe^0 materials (reference); (ii) reactors with Fe^0 materials (IS or SW) produced a more CH_4 amount (mL) compared with the reactor without Fe^0 materials (Fig. 4 (e) and (f)); (iii) reactors with IS materials (10 g/L IS) produced biogas with higher CH_4 (Fig. 4 (a)), H_2S (Fig. 4 (c)), and NH_3 (Fig. 4 (d)) but lower CO_2 (Fig. 4 (b)) contents compared with the reactor with SW materials (10 g/L SW); (iii) reactors with IS materials produced more CH_4 amount (mL) compared with the reactor with SW Fe^0 materials (Fig. 4 (e) and (f)))

Statistically, (i) there was a significant difference in the CH_4 content between biogas produced in 0 g/L (M = 53.2%, SD = 15%) and 10 g/L IS

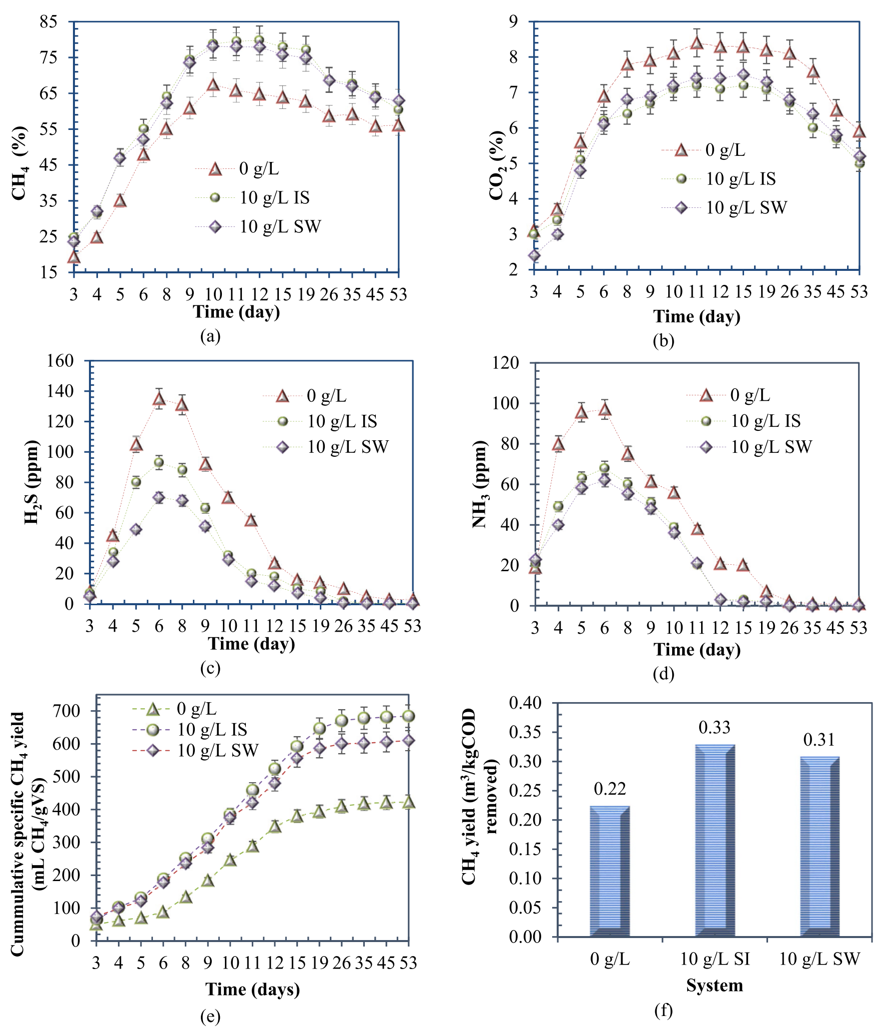

Fig. 4. Effects of Fe^0 types on biogas production: (a), (b), (c) and (d) are the variations in CH_4, CO_2, H_2S and NH_3 concentration, respectively; (e) cumulative specific CH_4 yield, and (f) CH_4 yield.

(M = 63.4%, SD = 17.30%), $t(14) = -11.4$, $p < 0.05$, two-tailed or 10 g/L SW (M = 62.3%, SD = 17.4%), $t(14) = -10.3$, $p < 0.05$, two-tailed. On the other hand, statistically, there was no distinguishable difference in the observed CH_4 content in the biogas between 10 g/L IS (M = 63.4%, SD = 17.30%) and 10 g/L SW (M = 62.3%, SD = 17.4%), $t(14) = -10.3$, $p > 0.05$, two-tailed (ii) there was a significant difference in the observed CO_2 content between biogas produced in 0 g/L (M = 6.5%, SD = 1.7%) and 10 g/L IS (M = 5.5%, SD = 1.4%), $t(14) = 8.9$, $p < 0.05$, two-tailed or 10 g/L SW (M = 5.6%, SD = 1.6%), $t(14) = 18.9$, $p < 0.05$, two-tailed. On the other hand, statistically, there was no distinguishable difference in the observed CO_2 content in the biogas between 10 g/L IS (M = 5.5%, SD = 1.4) and 10 g/L SW (M = 5.6%, SD = 1.6%), $t(14) = -1.0$, $p > 0.05$, two-tailed (iii) there was a significant difference in the observed H_2S content between biogas produced in 0 g/L (M = 47.9 ppm, SD = 47.6 ppm) and 10 g/L IS (M = 33.8 ppm, SD = 30.4 ppm), $t(14) = 4.3$, $p < 0.05$, two-tailed or 10 g/L SW (M = 22.6%, SD = 25.2%), $t(14) = 4.2$, $p < 0.05$, two-tailed. On the other hand, statistically, there was a significant difference in the observed H_2S content in the biogas between 10 g/L IS (M = 33.8 ppm, SD = 30.4 ppm) and 10 g/L SW (M = 25.2 ppm, SD = 22.6 ppm), $t(14) = 3.2$, $p < 0.05$, two-tailed (iv) there was a significant difference in the observed NH_3 content between biogas produced in 0 g/L (M = 38.3 ppm, SD = 36.0 ppm) and 10 g/L IS (M = 25.3 ppm, SD = 26.7 ppm), $t(14) = 4.3$, $p < 0.05$, two-tailed or 10 g/L SW (M = 23.4%, SD = 24.3%), $t(14) = 4.1$, $p < 0.05$, two-tailed. On the other hand, statistically, there was a significant difference in the observed NH_3 content in the biogas between 10 g/L IS (M = 25.3 ppm, SD = 26.7 ppm) and 10 g/L SW (M = 23.4%, SD = 24.3%), $t(14) = 2.5$, $p < 0.05$, two-tailed. The statistics suggest that; (i) dosing of Fe^0 materials in AD of DW increases the CH_4 content and decreases the CO_2, H_2S and NH_3 contents in biogas, (ii) addition of either IS or SW materials in Fe^0 - aided AD of DW will lead into the production of biogas with similar CH_4 and CO_2 but significantly different H_2S and NH_3 contents.

Biogas production with higher CH_4 yield and content in the reactors with Fe^0 compared to the reference reactor is perhaps due to the enhanced methanogenesis by Fe^0 materials [32,43,49,107–112]. For instance, compared to the 38.3% increase in CH_4 production reported in this study, it was reported elsewhere that dosing Fe^0 in the anaerobic treatment of wastewater increased CH_4 production by; 28% in brewery wastewater AD [113]; 26% in the AD of sulfate-rich wastewater [95]; 50% in cattle-dung slurry AD digestion [114]; 58% in the AD of cassava pulp and its wastewater [115]; 27%, 30%,40.4%, 46.1%, 117% and 120% in the digestion of sludge [65,97,98,116,117]; 230% in the digestion of cheese whey [96]; 74% in the digestion of palm oil mill wastewater [22]; 26.2, 52.6, 64.7, and 49.9% in the digestion of potato starch processing wastewater. Likewise, compared to the 12.4% increase in CH_4 content reported in this study, it was reported elsewhere that the addition of Fe^0 in the treatment of increased CH_4 content by; 6.93% in the sludge AD systems [118]; 5.1–13.2% in the digestion of wastewater sludge [65]; 40% in the digestion of cassava pulp and its wastewater [115].

The observed production of biogas with relatively lower CO_2 contents in the reactors dosed with Fe^0 materials compared to the reference reactor is perceivably due to the potentiality of Fe^0 materials to serve as an electron donor for reducing CO_2 to CH_4 as explained elsewhere [40,66,92,93]. Corrosion of Fe^0 materials releases H_2 (equation (1)) that is eventually utilized during the transformation of CO_2 to CH_4 (equation (3)) [40,119]. Compared to the 15.2% maximum decrease in CO_2 production reported in this study with 10 g/L IS, it was reported elsewhere that the addition of Fe^0 in the AD decreased CO_2 production by 58% in the AD of synthetic wastewater with 5 g/L dosage of nano-scale Fe^0 [113]; 25% in the AD of sulfate-rich wastewater with Fe^0 powder [95].

Lower H_2S content observed in biogas from Fe^0-aided reactors is possibly a result of Iron-Sulfide (FeS) precipitation (equation (2)) or a higher pH range (7.1–7.8) in the reactors with Fe^0 materials compared to the pH range (6.8–7.3) in the reference reactor (without Fe^0) as reported elsewhere [65–68,70,120]. In comparison with the 48.1% maximum decrease in H_2S production reported in this study with 10 g/L SW, it was reported elsewhere that the addition of Fe^0 in the AD decreased H_2S production by 98% in the AD of wastewater sludge with 0.10 wt% of nano-scale Fe^0 [65] and 50% in the AD of wastewater containing the sulfate [68].

The relatively lower NH_3 content in biogas from the reactors dosed with Fe^0 materials was perhaps due to the reactors' potential to convert available nitrogen more to N_2 and N_2O than to other forms (NH_4^+ or NH_3) [29] and precipitation of N as ($FeNH_4PO_4.H_2O$) [78–80]. The less NH_3 content in SW dosed reactor compared to IS reactor is perceivably due to the higher reactivity of SW compared to IS materials (section 2.1.2).

Compared to the 80% maximum decrease in NH_3 production with 10 g/L IS reported in this study, it was reported that the addition of zero valent Iron Scrap in the AD of sludge decreased NH_3 production by 82% compared to the reactor without Fe^0 materials [66].

The gaseous impurities (H_2S and NH_3) can be major problems in AD systems because of their potential to inhibit the AD process [121,122]. However, including Fe^0 in the AD of DW addresses this problem by producing biogas containing relatively fewer gaseous impurities (H_2S and NH_3) than without Fe^0 material.

3.3. *Kinetic study of methane production*

Table 7 and Fig. 5 present the observed and predicted cumulative CH_4 generation results and kinetic parameters of average cumulative CH_4 production curves. The cumulative CH_4 production for the 0 g/L (reference reactor), 10 g/L IS, and 10 g/L SW were: 422.6, 684.3, and 609.8 $mLCH_4/gVS$ for the observed data; 421.6, 700.6 and 618.1 $mLCH_4/gVS$ for Gompertz model; 434.0, 706.2 and 627.9 $mLCH_4/gVS$ for Logistic model; and 432.1, 695.5, and 618.8 $mLCH_4/gVS$ for Richard model. The higher cumulative CH_4 production observed in Fe^0-aided reactors for both experimental and predicted results is perceivably due to the potentiality of the materials to enhance methanogenesis, as described in Section 3.2.

Results presented in Table 7 indicate that the timeframe for the microbial adaptation and beginning of the production of biogas (lag phase, λ) is relatively shorter (≈2 days) for reactors dosed with Fe^0 materials compared to that (≈3 days) for the reference reactor. During the early seven days of the reactors' operation, relatively smaller drop in pH in Fe^0-aided reactors in comparison with the control (reactor without Fe^0 materials) as follows; the pH dropped from 7.3 to 6.8 in 0 g/L (reference reactor), 7.3 to 7.1 in 10 g/L IS, and 7.3 to 7.2 in 10 g/L SW reactors.

The pH drop may have been contributed by; the inoculum added to

Table 7
Kinetic parameters of average cumulative methane production curves.

Parameter	Model	0 g/L	10 g/L IS	10 g/L SW
CH_4 yield. V_0 ($mLCH_4/gVS$)	Experimental	422.6	684.3	609.8
CH_4 yield, A ($mLCH_4/gVS$)	Gompertz	421.6	700.6	618.1
	Logistic	434.0	706.2	627.9
	Richards	432.1	695.5	618.8
μ_m (mL/gVS/d)	Gompertz	49.3	62.0	62.5
	Logistic	48.7	70.7	59.8
	Richards	41.1	56.6	51.7
λ (days)	Gompertz	3.1	2.0	2.1
	Logistic	3.0	2.1	2.0
	Richards	3.1	2.0	2.0
ν	Gompertz	–	–	–
	Logistic	–	–	–
	Richards	2.3	2.4	2.4
R^2	Gompertz	0.997	0.969	0.994
	Logistic	0.933	0.964	0.960
	Richards	0.984	0.994	0.993
Difference between V_0 and A (%)	Gompertz	0.25	2.37	1.37
	Logistic	2.68	3.20	2.98
	Richards	2.23	1.63	1.48

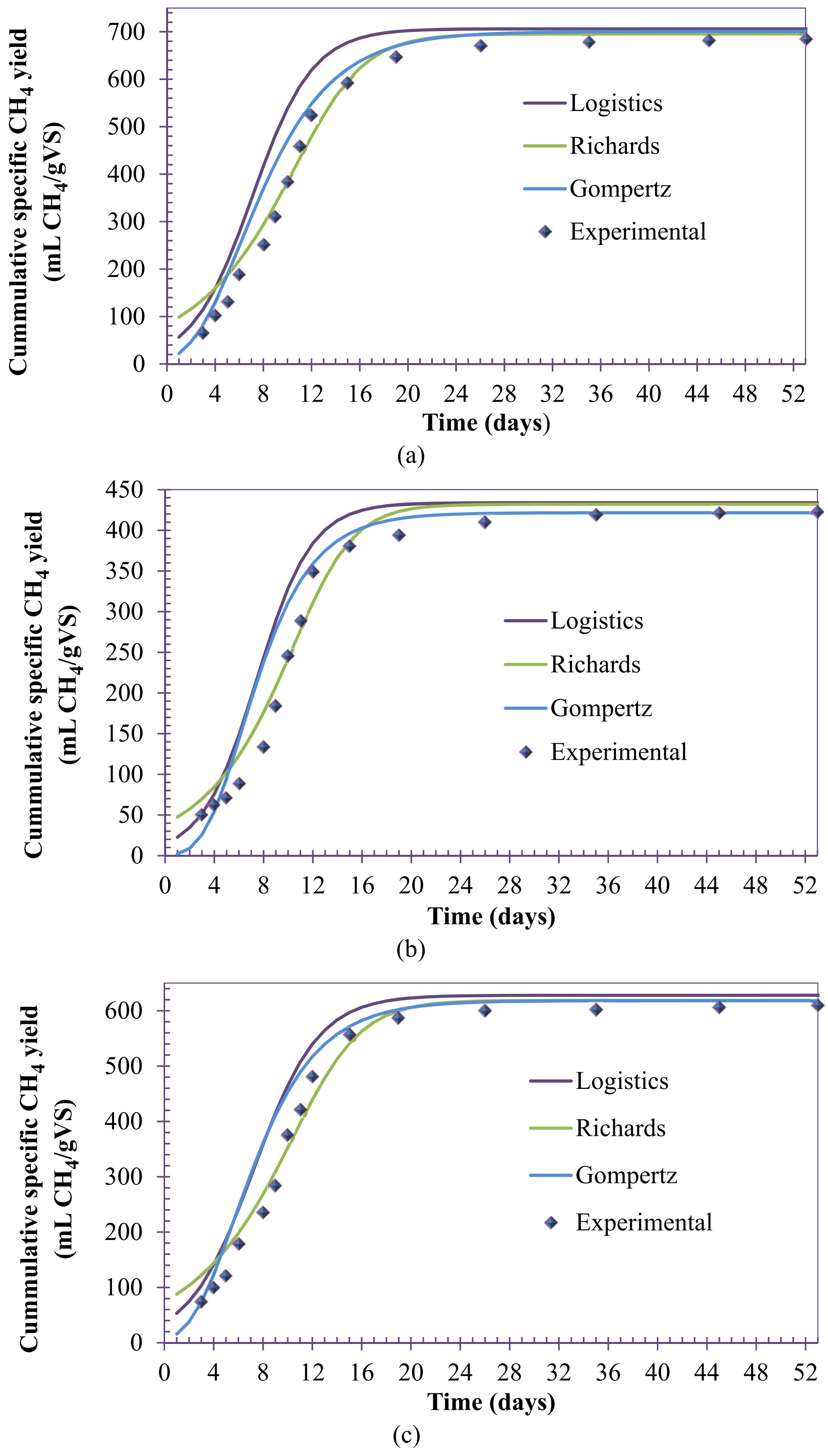

Fig. 5. Cumulative experimental methane production and their fit with models: (a) 0 g/L (control); (b) 10 g/L IS and (c) 10 g/L SW reactors.

the systems and the second stage of AD (acidogenesis) associated with the production of volatile fatty acids (VFA), especially butyrate, propionate, and valerate [5]. Accumulation of VFA has been mentioned as one of the causes of prolonged lag phases in AD [123]. Besides, it has been reported elsewhere [124] that good buffering capacity at the starting stages of AD reduces the lag phase. Similarly, the beginning pH influenced the latency period (λ) in the AD of vinasse, whereby the best condition for biogas production was observed at initial pH of 7 [125]. Therefore, for the reactors dosed with Fe^0 materials, neutralization occurs for a part of hydroxyl iron (OH^-) released in the time of anaerobic oxidation of Fe^0 (Equation (1)); because of that, the pH was accordingly regulated in the reactors. Perceivably, the pH regulation by Fe^0 materials contributed to a relatively shorter time taken by microbes to adapt and start the generation of CH_4 in the reactors dosed with Fe^0 materials than in the reference reactor (0 g/L).

For the reference reactor (0 g/L), the difference between the observed (V_0) and predicted (A) biogas yield was 0.25% for the modified Gompertz model, which is less than 2.23% for Richards or 2.68% for the Logistic model (Table 7). Thus, among the tested models, the modified Gompertz was magnificent for modelling CH_4 production in the AD of

DW since the model gave the lowest difference between V_0 and A. On the other hand, for 10 g/L IS reactor, the difference between the observed and predicted biogas yield was 1.63% for the Richard model, which is less than 2.37% for Gompertz or 3.20% for the Logistic model.

Thus, among the tested models, the Richard model was the best model for predicting CH_4 production in the Iron Scrap-aided AD of DW. Furthermore, for 10 g/L SW reactor, the difference between the observed and predicted biogas yield was 1.37% for the Gompertz model, which is less than 1.48% for Richards or 2.98% for the Logistic model. Thus, among the tested models, the modified Gompertz was magnificent for modelling CH_4 production in the steel wool-aided AD of DW. However, the fitting error of equal or less than 10% between the observed and predicted biogas yield has been considered a good fitting error in various studies [126–128]. Therefore, based on the results presented in Table 7, all the tested models (Gompertz, Logistic and Richard) generally portrayed good fitting error (error <10%) in predicting CH_4 production in Fe^0 - aided AD of DW. However, generally, the Richard was the best model for predicting CH_4 production from Fe^0 (IS and SW) - aided AD of DW with the lowest fitting error ranging from 1.63 to 1.48% compared to 1.37–2.37% for Gompertz or 2.98–3.20% for Logistic model (Table 7).

4. Conclusion

Compared with the reactor without Fe^0 (reference), the Fe^0 -aided AD of DW enriched CH_4 of biogas (potential for energy recovery) by 12.4% with IS and 11.5% with SW. The Fe^0 dosed reactors produced sludge with relatively higher nutrients and toxic elements concentrations. However, the concentrations of toxic elements are far less than the EPA recommended ceiling limits for land application. Moreover, the Fe^0-aided AD produced well-settling sludge (SVI <100). Furthermore, more than 80% of solids produced from Fe^0-aided AD of DW can be removed using sedimentation tanks designed at an overflow rate ≤40 m/d. Statistically, dosing either IS or SW materials in AD of DW will lead to the production of biogas with similar CH_4 (79.8% for IS and 78.9% for SW), but significantly different H_2S (93 ppm for IS and 70 ppm for SW) and NH_3 (68 ppm for IS and 62 ppm for SW) contents. Therefore, although this study suggests that including either SW or IS can address the AD inhibition problem caused by H_2S and NH_3 by producing biogas containing relatively fewer gaseous impurities (H_2S and NH_3), SW will perform better perceivably due to its higher reactivity compared to IS. On the other hand, Richard was the best model for predicting CH_4 production from Fe^0-aided AD of DW. As limitations, this research did not consider; (i) the effects of varying the sizes of Fe^0 materials, (ii) the effects of the materials on the dewaterability of the resulting sludge, and (iii) the economic significance of applying Fe^0 materials in AD of DW. Therefore, the authors consider the limitations as the motive for continuing this study.

Declaration of competing interest

The authors declare that they have no known competing financial interests or personal relationships that could have appeared to influence the work reported in this paper.

Data availability

Data will be made available on request.

Acknowledgement

The Mbeya University of Science and Technology (MUST) supported this research financially.

References

[1] H. Gijzen, Anaerobes, aerobes and phototrophs (A winning team for wastewater management), Water Sci. Technol. 44 (8) (2001) 123–132.
[2] H. Gijzen, Anaerobic digestion for sustainable development: a natural approach, Water Sci. Technol. 45 (10) (2002) 321–328.
[3] N.F. Gray, Biology of Wastewater Treatment, second ed. Vol. 4, World Scientific, 2004.
[4] J.C. Akunna, Anaerobic Waste-Wastewater Treatment and Biogas Plants: a Practical Handbook, CRC Press, 2018.
[5] G. Tchobanoglous, H.D. Stensel, R. Tsuchihashi, F. Burton, M. Abu-Orf, G. Bowden, W. Pfrang, Wastewater Engineering: Treatment and Resource Recovery, fifth ed., McGraw-Hill Education, 2014.
[6] S. Moran, An Applied Guide to Water and Effluent Treatment Plant Design, Butterworth-Heinemann, 2018.
[7] K. Kujawa-Roeleveld, G. Zeeman, Anaerobic treatment in decentralised and source-separation-based sanitation concepts, Rev. Environ. Sci. Biotechnol. 5 (1) (2006) 115–139, https://doi.org/10.1007/s11157-005-5789-9.
[8] C. Augustos de Lemos Chernicharo, M. Von Sperling, Biological Wastewater Treatment in Warm Climate Regions, IWA publishing, 2005.
[9] A. Hendriks, G. Zeeman, Pretreatments to enhance the digestibility of lignocellulosic biomass, Bioresour. Technol. 100 (1) (2009) 10–18, https://doi.org/10.1016/j.biortech.2008.05.027.
[10] F.A. Shah, Q. Mahmood, N. Rashid, A. Pervez, I.A. Raja, M.M. Shah, Co-digestion, pretreatment and digester design for enhanced methanogenesis, Renew. Sustain. Energy Rev. 42 (2015) 627–642, https://doi.org/10.1016/j.rser.2014.10.053.
[11] R. Karki, W. Chuenchart, K. Surendra, S. Shrestha, L. Raskin, S. Sung, A. Hashimoto, S.K. Khanal, Anaerobic co-digestion: current status and perspectives, Bioresour. Technol. 330 (2021), 125001, https://doi.org/10.1016/j.biortech.2021.125001.
[12] M. Romero-Güiza, J. Vila, J. Mata-Alvarez, J. Chimenos, S. Astals, The role of additives on anaerobic digestion: a review, Renew. Sustain. Energy Rev. 58 (2016) 1486–1499, https://doi.org/10.1016/j.rser.2015.12.094.
[13] Z.H. Farooqi, R. Begum, K. Naseem, W. Wu, A. Irfan, Zero valent iron nanoparticles as sustainable nanocatalysts for reduction reactions, Catal. Rev. 64 (2) (2022) 286–355, https://doi.org/10.1080/01614940.2020.1807797.
[14] N. Izadi, B.H. Ali, M.S. Shahin, M. Baghdadi, The removal of Cr (VI) from aqueous and saturated porous media by nanoscale zero-valent iron stabilized with flaxseed gum extract: synthesis by continuous flow injection method, Kor. J. Chem. Eng. 39 (2022) 2217–2228, https://doi.org/10.1007/s11814-022-1069-4.
[15] Y. Li, X. Guo, H. Dong, X. Luo, X. Guan, X. Zhang, X. Xia, Selenite removal from groundwater by zero-valent iron (ZVI) in combination with oxidants, Chem. Eng. J. 345 (2018) 432–440, https://doi.org/10.1016/j.cej.2018.03.187.
[16] Y. Liu, J. Wang, Reduction of nitrate by zero valent iron (ZVI)-based materials: a review, Sci. Total Environ. 671 (2019) 388–403, https://doi.org/10.1016/j.scitotenv.2019.03.317.
[17] N.R. Mucha, Electrospun carbon nanofibers with surface attached zero valent iron nanoparticles for heavy metal remediation in ground and wastewater, in: Nanoengineering, North Carolina Agricultural and Technical State University, 2016.
[18] Y. Zang, Y. Yang, Y. Hu, H.H. Ngo, X.C. Wang, Y.-Y. Li, Zero-valent iron enhanced anaerobic digestion of pre-concentrated domestic wastewater for bioenergy recovery: characteristics and mechanisms, Bioresour. Technol. 310 (2020), 123441, https://doi.org/10.1016/j.biortech.2020.123441.
[19] Y. Feng, Y. Zhang, X. Quan, S. Chen, Enhanced anaerobic digestion of waste activated sludge digestion by the addition of zero valent iron, Water Res. 52 (2014) 242–250, https://doi.org/10.1016/j.watres.2013.10.072.
[20] X. Kong, Y. Wei, S. Xu, J. Liu, H. Li, Y. Liu, S. Yu, Inhibiting excessive acidification using zero-valent iron in anaerobic digestion of food waste at high organic load rates, Bioresour. Technol. 211 (2016) 65–71, https://doi.org/10.1016/j.biortech.2016.03.078.
[21] T. Yuan, S. Bian, J.H. Ko, J. Liu, X. Shi, Q. Xu, Exploring the roles of zero-valent iron in two-stage food waste anaerobic digestion, Waste Manag. 107 (2020) 91–100, https://doi.org/10.1016/j.wasman.2020.04.004.
[22] V. Domrongpokkaphan, C. Phalakornkule, M. Khemkhao, In-situ methane enrichment of biogas from anaerobic digestion of palm oil mill effluent by addition of zero valent iron (ZVI), Int. J. Hydrogen Energy 46 (60) (2021) 30976–30987, https://doi.org/10.1016/j.ijhydene.2021.03.083.
[23] D. Wu, S. Zheng, A. Ding, G. Sun, M. Yang, Performance of a zero valent iron-based anaerobic system in swine wastewater treatment, J. Hazard Mater. 286 (2015) 1–6, https://doi.org/10.1016/j.jhazmat.2014.12.029.
[24] Y. Zhang, Y. Jing, X. Quan, Y. Liu, P. Onu, A built-in zero valent iron anaerobic reactor to enhance treatment of azo dye wastewater, Water Sci. Technol. 63 (4) (2011) 741–746, https://doi.org/10.2166/wst.2011.301.
[25] S. Deng, S. Peng, B. Xie, X. Yang, S. Sun, H. Yao, D. Li, Influence characteristics and mechanism of organic carbon on denitrification, N2O emission and NO2− accumulation in the iron [Fe (0)]-oxidizing supported autotrophic denitrification process, Chem. Eng. J. 393 (2020), 124736, https://doi.org/10.1016/j.cej.2020.124736.
[26] A.F. Florea, C. Lu, H.C.B. Hansen, A zero-valent iron and zeolite filter for nitrate recycling from agricultural drainage water, Chemosphere 287 (2022), 131993, https://doi.org/10.1016/j.chemosphere.2021.131993.
[27] G. Hua, M.W. Salo, C.G. Schmit, C.H. Hay, Nitrate and phosphate removal from agricultural subsurface drainage using laboratory woodchip bioreactors and recycled steel byproduct filters, Water Res. 102 (2016) 180–189, https://doi.org/10.1016/j.watres.2016.06.022.

[28] B. Konadu-Amoah, R. Hu, A.I. Ndé-Tchoupé, W. Gwenzi, C. Noubactep, Metallic iron (Fe0)-based materials for aqueous phosphate removal: a critical review, J. Environ. Manag. 315 (2022), 115157, https://doi.org/10.1016/j.jenvman.2022.115157.

[29] B.A. Till, L.J. Weathers, P.J. Alvarez, Fe (0)-supported autotrophic denitrification, Environ. Sci. Technol. 32 (5) (1998) 634–639, https://doi.org/10.1021/es9707769.

[30] Y. Liu, Y. Zhang, X. Quan, Y. Li, Z. Zhao, X. Meng, S. Chen, Optimization of anaerobic acidogenesis by adding Fe0 powder to enhance anaerobic wastewater treatment, Chem. Eng. J. 192 (2012) 179–185, https://doi.org/10.1016/j.cej.2012.03.044.

[31] X. Meng, Y. Zhang, Q. Li, X. Quan, Adding Fe0 powder to enhance the anaerobic conversion of propionate to acetate, Biochem. Eng. J. 73 (2013) 80–85, https://doi.org/10.1016/j.bej.2013.02.004.

[32] J. Zhang, Y. Qu, Q. Qi, P. Zhang, Y. Zhang, Y.W. Tong, Y. He, The bio-chemical cycle of iron and the function induced by ZVI addition in anaerobic digestion: a review, Water Res. 186 (2020), 116405, https://doi.org/10.1016/j.watres.2020.116405.

[33] Y. Zhang, Y. Feng, X. Quan, Zero-valent iron enhanced methanogenic activity in anaerobic digestion of waste activated sludge after heat and alkali pretreatment, Waste Manag. 38 (2015) 297–302, https://doi.org/10.1016/j.wasman.2015.01.036.

[34] N. Boontian, Effect of zero valent iron (ZVI) in wastewater treatment: a review, in: Applied Mechanics and Materials, Trans Tech Publ, 2015. https://doi.org/10.4028/www.scientific.net/AMM.775.180.

[35] Y. Zhong, J. He, P. Zhang, X. Zou, X. Pan, J. Zhang, Effects of different particle size of zero-valent iron (ZVI) during anaerobic digestion: performance and mechanism from genetic level, Chem. Eng. J. 435 (2022), 134977, https://doi.org/10.1016/j.cej.2022.134977.

[36] Y. Liu, Y. Zhang, B.-J. Ni, Zero valent iron simultaneously enhances methane production and sulfate reduction in anaerobic granular sludge reactors, Water Res. 75 (2015) 292–300, https://doi.org/10.1016/j.watres.2015.02.056.

[37] Y. Liu, Q. Wang, Y. Zhang, B.-J. Ni, Zero valent iron significantly enhances methane production from waste activated sludge by improving biochemical methane potential rather than hydrolysis rate, Sci. Rep. 5 (2015) 8263, https://doi.org/10.1038/srep08263.

[38] N. Ren, H. Chua, S. Chan, Y.F. Tsang, Y. Wang, N. Sin, Assessing optimal fermentation type for bio-hydrogen production in continuous-flow acidogenic reactors, Bioresour. Technol. 98 (9) (2007) 1774–1780, https://doi.org/10.1016/j.biortech.2006.07.026.

[39] Y. Hwang, P. Sivagurunathan, M.-K. Lee, Y.-M. Yun, Y.-C. Song, D.-H. Kim, Enhanced hydrogen fermentation by zero valent iron addition, Int. J. Hydrogen Energy 44 (6) (2019) 3387–3394, https://doi.org/10.1016/j.ijhydene.2018.06.015.

[40] L. Ma, L. Zhou, S.M. Mbadinga, J.-D. Gu, B.-Z. Mu, Accelerated CO2 reduction to methane for energy by zero valent iron in oil reservoir production waters, Energy 147 (2018) 663–671, https://doi.org/10.1016/j.energy.2018.01.087.

[41] C. Ou, J. Shen, S. Zhang, Y. Mu, W. Han, X. Sun, J. Li, L. Wang, Coupling of iron shavings into the anaerobic system for enhanced 2, 4-dinitroanisole reduction in wastewater, Water Res. 101 (2016) 457–466, https://doi.org/10.1016/j.watres.2016.06.002.

[42] K. Bensaida, R. Eljamal, Y. Sughihara, O. Eljamal, The impact of iron bimetallic nanoparticles on bulk microbial growth in wastewater, J. Water Proc. Eng. 40 (2021), 101825, https://doi.org/10.1016/j.jwpe.2020.101825.

[43] N. Boontian, Effect of zero valent iron (ZVI) in wastewater treatment: a review, Appl. Mech. Mater. 775 (2015) 180–184. https://doi.org/10.4028/www.scientific.net/AMM.775.180.

[44] F. Fu, D.D. Dionysiou, H. Liu, The use of zero-valent iron for groundwater remediation and wastewater treatment: a review, J. Hazard Mater. 267 (2014) 194–205, https://doi.org/10.1016/j.jhazmat.2013.12.062.

[45] N. Ahmed, D. Vione, L. Rivoira, L. Carena, M. Castiglioni, M.C. Bruzzoniti, A review on the degradation of pollutants by Fenton-Like systems based on Zero-Valent iron and persulfate: effects of reduction potentials, pH, and anions occurring in waste waters, Molecules 26 (15) (2021) 4584, https://doi.org/10.3390/molecules26154584.

[46] K. Plessl, A. Russ, D. Vollprecht, Application and development of zero-valent iron (ZVI) for groundwater and wastewater treatment, Int. J. Environ. Sci. Technol. (2022) 1–16, https://doi.org/10.1007/s13762-022-04536-7.

[47] X. Shi, W. Wei, L. Wu, B.-J. Ni, Zero-valent iron mediated biological wastewater and sludge treatment, Chem. Eng. J. 426 (2021), 130821, https://doi.org/10.1016/j.cej.2021.130821.

[48] W. Wang, P. Zhao, Y. Hu, R. Zan, Application of weak magnetic field coupling with zero-valent iron for remediation of groundwater and wastewater: a review, J. Clean. Prod. 262 (2020), 121341, https://doi.org/10.1016/j.jclepro.2020.121341.

[49] Y. Xu, C. Wang, J. Hou, P. Wang, G. You, L. Miao, B. Lv, Y. Yang, F. Zhang, Application of zero valent iron coupling with biological process for wastewater treatment: a review, Rev. Environ. Sci. Biotechnol. 16 (4) (2017) 667–693, https://doi.org/10.1007/s11157-017-9445-y.

[50] G. You, P. Wang, J. Hou, C. Wang, Y. Xu, L. Miao, B. Lv, Y. Yang, F. Zhang, The use of zero-valent iron (ZVI)–microbe technology for wastewater treatment with special attention to the factors influencing performance: a critical review, Crit. Rev. Environ. Sci. Technol. 47 (10) (2017) 877–907, https://doi.org/10.1080/10643389.2017.1334457.

[51] I.M. Lo, R.Y. Surampalli, K.C. Lai, Zero-valent Iron Reactive Materials for Hazardous Waste and Inorganics Removal, United States of America: American Society of civil engineers, 2006, https://doi.org/10.1061/9780784408810.

[52] G.K. Kafle, S.-H. Kim, Kinetic study of the anaerobic digestion of swine manure at mesophilic temperature: a lab scale batch operation, J. Biosyst. Eng. 37 (4) (2012) 233–244, https://doi.org/10.5307/JBE.2012.37.4.233.

[53] M.A. Mohamed, D. Nourou, B. Boudy, N. Mamoudou, Theoretical models for prediction of methane production from anaerobic digestion: a critical review, Int. J. Phys. Sci. 13 (13) (2018) 206–216, https://doi.org/10.5897/IJPS2018.4740.

[54] Y. Pererva, C.D. Miller, R.C. Sims, Existing empirical kinetic models in biochemical methane potential (BMP) testing, their selection and numerical solution, Water 12 (6) (2020) 1831, https://doi.org/10.3390/w12061831.

[55] A. Ware, N. Power, Modelling methane production kinetics of complex poultry slaughterhouse wastes using sigmoidal growth functions, Renew. Energy 104 (2017) 50–59, https://doi.org/10.1016/j.renene.2016.11.045.

[56] M. Lufingo, A.I. Ndé-Tchoupé, R. Hu, K.N. Njau, C. Noubactep, A novel and facile method to characterize the suitability of metallic iron for water treatment, Water 11 (12) (2019) 2465, https://doi.org/10.3390/w11122465.

[57] C. Noubactep, G. Meinrath, P. Dietrich, M. Sauter, B.J. Merkel, Testing the suitability of zerovalent iron materials for reactive walls, Environ. Chem. 2 (1) (2005) 71–76, https://doi.org/10.1071/EN04014.

[58] R. Hu, X. Cui, M. Xiao, P. Qiu, M. Lufingo, W. Gwenzi, C. Noubactep, Characterizing the suitability of granular Fe0 for the water treatment industry, Processes 7 (10) (2019) 652, https://doi.org/10.3390/pr7100652.

[59] O. Bakari, K.N. Njau, C. Noubactep, Fe0-Supported anaerobic digestion for organics and nutrients removal from domestic sewage, Water 14 (10) (2022) 1623, https://doi.org/10.3390/w14101623.

[60] C. Noubactep, The fundamental mechanism of aqueous contaminant removal by metallic iron, WaterSA 36 (5) (2010) 663–670, https://doi.org/10.10520/EJC116733.

[61] B. Konadu-Amoah, A.I. Ndé-Tchoupé, R. Hu, W. Gwenzi, C. Noubactep, Investigating the Fe0/H2O systems using the methylene blue method: validity, applications, and future directions, Chemosphere 291 (2022), 132913, https://doi.org/10.1016/j.chemosphere.2021.132913.

[62] C. Noubactep, A. Schöner, Metallic iron for environmental remediation: learning from electrocoagulation, J. Hazard Mater. 175 (1–3) (2010) 1075–1080, https://doi.org/10.1016/j.jhazmat.2009.09.152.

[63] USEPA, A Guide for Land Appliers on the Requirements of the Federal Standards for the Use or Disposal of Sewage Sludge, vol. 40, 1994, p. 105. CFR Part 503.

[64] E. Wiśniowska, A. Grobelak, P. Kokot, M. Kacprzak, Sludge legislation-comparison between different countries, Industrial and municipal sludge (2019) 201–224, https://doi.org/10.1016/B978-0-12-815907-1.00010-6.

[65] L. Su, X. Shi, G. Guo, A. Zhao, Y. Zhao, Stabilization of sewage sludge in the presence of nanoscale zero-valent iron (nZVI): abatement of odor and improvement of biogas production, J. Mater. Cycles Waste Manag. 15 (4) (2013) 461–468, https://doi.org/10.1007/s10163-013-0150-9.

[66] N. Lytras, M. Andronikou, G. Chrysanthou, M. Stylianou, A. Agapiou, I. Vyrides, Ex-situ biogas upgrading to methane and removal of VOCs in a system of zero valent iron and anaerobic granular sludge, Res. Square (2021) PPR357882, https://doi.org/10.21203/rs.3.rs-546207/v1.

[67] R. Ruan, J. Cao, C. Li, D. Zheng, J. Luo, The influence of micro-oxygen addition on desulfurization performance and microbial communities during waste-activated sludge digestion in a rusty scrap iron-loaded anaerobic digester, Energies 10 (2) (2017) 258, https://doi.org/10.3390/en10020258.

[68] J. Zhang, Y. Zhang, X. Quan, Y. Liu, X. An, S. Chen, H. Zhao, Bioaugmentation and functional partitioning in a zero valent iron-anaerobic reactor for sulfate-containing wastewater treatment, Chem. Eng. J. 174 (1) (2011) 159–165, https://doi.org/10.1016/j.cej.2011.08.069.

[69] X. Flores-Alsina, K. Solon, C.K. Mbamba, S. Tait, K.V. Gernaey, U. Jeppsson, D. J. Batstone, Modelling phosphorus (P), sulfur (S) and iron (Fe) interactions for dynamic simulations of anaerobic digestion processes, Water Res. 95 (2016) 370–382, https://doi.org/10.1016/j.watres.2016.03.012.

[70] J.V.A.H.N. Thorkild Hvitved-Jacobsen, Sewer Processes: Microbial and Chemical Process Engineering of Sewer Networks, second ed., CRC press, 2013.

[71] N. Booker, A. Priestley, I. Fraser, Struvite formation in wastewater treatment plants: opportunities for nutrient recovery, Environ. Technol. 20 (7) (1999) 777–782, https://doi.org/10.1080/09593332008616874.

[72] K. Zhou, B. Wu, X. Dai, X. Chai, Development of polymeric iron/zirconium-pillared clinoptilolite for simultaneous removal of multiple inorganic contaminants from wastewater, Chem. Eng. J. 347 (2018) 819–827, https://doi.org/10.1016/j.cej.2018.04.104.

[73] G. Bridger, M.L. Salutsky, R. Starostka, Micronutrient sources, metal ammonium phosphates as fertilizers, J. Agric. Food Chem. 10 (3) (1962) 181–188, https://doi.org/10.1021/jf60121a006.

[74] T. Pullen, Anaerobic Digestion-Making Biogas-Making Energy, first ed., Routledge, London, 2015.

[75] P.L. McCarty, J. Bae, J. Kim, Domestic wastewater treatment as a net energy producer–can this be achieved? Environ. Sci. Technol. 45 (17) (2011) 7100–7106, https://doi.org/10.1021/es2014264.

[76] R. Hu, A.I. Ndé-Tchoupé, M. Lufingo, M. Xiao, A. Nassi, C. Noubactep, K.N. Njau, The impact of selected pretreatment procedures on iron dissolution from metallic iron specimens used in water treatment, Sustainability 11 (3) (2019) 671, https://doi.org/10.3390/su11030671.

[77] Y.-M. Chen, C.-W. Li, S.-S. Chen, Fluidized zero valent iron bed reactor for nitrate removal, Chemosphere 59 (6) (2005) 753–759, https://doi.org/10.1016/j.chemosphere.2004.11.020.

[78] P. Antwi, J. Li, P.O. Boadi, J. Meng, E. Shi, X. Chi, K. Deng, F. Ayivi, Dosing effect of zero valent iron (ZVI) on biomethanation and microbial community distribution as revealed by 16S rRNA high-throughput sequencing, Int. Biodeterior. Biodegrad. 123 (2017) 191–199, https://doi.org/10.1016/j.ibiod.2017.06.022.
[79] L. Zhao, Y. Ji, D. Kong, J. Lu, Q. Zhou, X. Yin, Simultaneous removal of bisphenol A and phosphate in zero-valent iron activated persulfate oxidation process, Chem. Eng. J. 303 (2016) 458–466, https://doi.org/10.1016/j.scitotenv.2021.149667.
[80] R. Riffat, T. Husnain, Fundamentals of Wastewater Treatment and Engineering, Crc Press, 2013.
[81] S.R. Qasim, G. Zhu, Wastewater Treatment and Reuse, Theory and Design Examples, in: Principles and Basic Treatment, ume 1, CRC Press, 2017.
[82] M.L. Davis, Water and Wastewater Engineering: Design Principles and Practice, McGraw-Hill Education, 2010.
[83] R. Weiner, R. Matthews, P.A. Vesilind, Environmental Engineering, Butterworth-Heinemann, 2003.
[84] C. Zhao, H. Mu, Y. Zhao, L. Wang, B. Zuo, Microbial characteristics analysis and kinetic studies on substrate composition to methane after microbial and nutritional regulation of fruit and vegetable wastes anaerobic digestion, Bioresour. Technol. 249 (2018) 315–321, https://doi.org/10.1016/j.biortech.2017.10.041.
[85] M. Bakraoui, F. Karouach, B. Ouhammou, M. Aggour, A. Essamri, H. El Bari, Kinetics study of the methane production from experimental recycled pulp and paper sludge by CSTR technology, J. Mater. Cycles Waste Manag. 21 (6) (2019) 1426–1436, https://doi.org/10.1007/s10163-019-00894-6.
[86] D. Puyol, X. Flores-Alsina, Y. Segura, R. Molina, B. Padrino, J. Fierro, K. Gernaey, J. Melero, F. Martinez, Exploring the effects of ZVI addition on resource recovery in the anaerobic digestion process, Chem. Eng. J. 335 (2018) 703–711, https://doi.org/10.1016/j.cej.2017.11.029.
[87] D. Mamais, P.A. Pitt, Y.W. Cheng, J. Loiacono, D. Jenkins, Determination of ferric chloride dose to control struvite precipitation in anaerobic sludge digesters, Water Environ. Res. 66 (7) (1994) 912–918, https://doi.org/10.2175/WER.66.7.8.
[88] R. Eljamal, I. Kahraman, O. Eljamal, I.P. Thompson, I. Maamoun, G. Yilmaz, Impact of nZVI on the formation of aerobic granules, bacterial growth and nutrient removal using aerobic sequencing batch reactor, Environ. Technol. Innov. 19 (2020), 100911, https://doi.org/10.1016/j.eti.2020.100911.
[89] D.A. Cornwell, Introduction to Environmental Engineering, sixth ed., McGraw Hill LLC, New York, NY 10019, 2022, 1325 Avenue of the Americas.
[90] P.A. Vesilind, S.M. Morgan, L.G. Heine, Introduction to Environmental Engineering, third ed., Cengage Learning, CT 06902 USA, 2009, 200 First Stamford Place, Suite 400 Stamford,.
[91] C.D. Filipe, C.L. Grady Jr., Biological Wastewater Treatment, Revised and Expanded, Crc Press, 1998.
[92] E. Abdelsalam, M. Samer, Y. Attia, M. Abdel-Hadi, H. Hassan, Y. Badr, Influence of zero valent iron nanoparticles and magnetic iron oxide nanoparticles on biogas and methane production from anaerobic digestion of manure, Energy 120 (2017) 842–853, https://doi.org/10.1016/j.energy.2016.11.137.
[93] N. Belay, L. Daniels, Elemental metals as electron sources for biological methane formation from CO2, Antonie Leeuwenhoek 57 (1) (1990) 1–7, https://doi.org/10.1007/BF00400329.
[94] Y. Konaté, A.H. Maiga, C. Casellas, B. Picot, Biogas production from an anaerobic pond treating domestic wastewater in Burkina Faso, Desalination Water Treat. 51 (10–12) (2013) 2445–2452, https://doi.org/10.1080/19443994.2012.747642.
[95] N. Paepatung, W. Songkasiri, H. Yasui, C. Phalakornkule, Enhancing methanogenesis in fed-batch anaerobic digestion of high-strength sulfate-rich wastewater using zero valent scrap iron, J. Environ. Chem. Eng. 8 (6) (2020), 104508, https://doi.org/10.1016/j.jece.2020.104508.
[96] P. Charalambous, I. Vyrides, In situ biogas upgrading and enhancement of anaerobic digestion of cheese whey by addition of scrap or powder zero-valent iron (ZVI), J. Environ. Manag. 280 (2021), 111651, https://doi.org/10.1016/j.jenvman.2020.111651.
[97] W. Wei, Z. Cai, J. Fu, G.-J. Xie, A. Li, X. Zhou, B.-J. Ni, D. Wang, Q. Wang, Zero valent iron enhances methane production from primary sludge in anaerobic digestion, Chem. Eng. J. 351 (2018) 1159–1165, https://doi.org/10.1016/j.cej.2018.06.160.
[98] Y. Liu, Q. Wang, Y. Zhang, B.-J. Ni, Zero valent iron significantly enhances methane production from waste activated sludge by improving biochemical methane potential rather than hydrolysis rate, Sci. Rep. 5 (1) (2015) 1–6, https://doi.org/10.1038/srep08263.
[99] C.M. Dykstra, S.G. Pavlostathis, Zero-valent iron enhances biocathodic carbon dioxide reduction to methane, Environ. Sci. Technol. 51 (21) (2017) 12956–12964, https://doi.org/10.1021/acs.est.7b02777.
[100] N. Sleiman, V. Deluchat, M. Wazne, M. Mallet, A. Courtin-Nomade, V. Kazpard, M. Baudu, Phosphate removal from aqueous solutions using zero valent iron (ZVI): influence of solution composition and ZVI aging, Colloids Surf. A Physicochem. Eng. Asp. 514 (2017) 1–10, https://doi.org/10.1016/j.colsurfa.2016.11.014.
[101] S. Li, Y. Ding, W. Wang, H. Lei, A facile method for determining the Fe (0) content and reactivity of zero valent iron, Anal. Methods 8 (6) (2016) 1239–1248, https://doi.org/10.1039/C5AY02182K.
[102] H. Alidadi, A. Najafpoor, A. Parvaresh, Determination of carbon/nitrogen ratio and heavy metals in bulking agents used for sewage composting, Pakistan J. Biol. Sci. 10 (22) (2007) 4180–4182, https://doi.org/10.3923/pjbs.2007.4180.4182.
[103] H. Lin, J. Gan, A. Rajendran, C.E.R. Reis, B. Hu, Phosphorus removal and recovery from digestate after biogas production, in: Biofuels-status and Perspective, IntechOpen, 2015, https://doi.org/10.5772/60474.
[104] T. Almeelbi, A. Bezbaruah, Aqueous phosphate removal using nanoscale zero-valent iron, in: Nanotechnology for Sustainable Development, Springer, Cham, 2012, pp. 197–210, https://doi.org/10.1007/978-3-319-05041-6_16.
[105] Q. Wang, Z. Liao, D. Yao, Z. Yang, Y. Wu, C. Tang, Phosphorus immobilization in water and sediment using iron-based materials: a review, Sci. Total Environ. 767 (2021), 144246, https://doi.org/10.1016/j.scitotenv.2020.144246.
[106] R.T. Wilkin, M.S. McNeil, Laboratory evaluation of zero-valent iron to treat water impacted by acid mine drainage, Chemosphere 53 (7) (2003) 715–725, https://doi.org/10.1016/S0045-6535(03)00512-5.
[107] M. Liu, Y. Wei, X. Leng, Improving biogas production using additives in anaerobic digestion: a review, J. Clean. Prod. 297 (2021), 126666, https://doi.org/10.1016/j.jclepro.2021.126666.
[108] W. Ye, J. Lu, J. Ye, Y. Zhou, The effects and mechanisms of zero-valent iron on anaerobic digestion of solid waste: a mini-review, J. Clean. Prod. 278 (2021), 123567, https://doi.org/10.1016/j.jclepro.2020.123567.
[109] L. Zhang, A. Kuroki, Y.W. Tong, A mini-review on in situ biogas upgrading technologies via enhanced hydrogenotrophic methanogenesis to improve the quality of biogas from anaerobic digesters, Front. Energy Res. 8 (2020) 69.
[110] M.A. Ganzoury, N.K. Allam, Impact of nanotechnology on biogas production: a mini-review, Renew. Sustain. Energy Rev. 50 (2015) 1392–1404.
[111] W. Ma, H. Xin, D. Zhong, F. Qian, H. Han, Y. Yuan, Effects of different states of Fe on anaerobic digestion: a review, J. Harbin Inst. Technol. 22 (2015) 69–75, https://doi.org/10.11916/j.issn.1005-9113.2015.06.010.
[112] J. Zhao, Y. Li, R. Dong, Recent Progress towards In-Situ Biogas Upgrading Technologies, vol. 800, Science of The Total Environment, 2021, 149667, https://doi.org/10.1016/j.scitotenv.2021.149667.
[113] A.W. Carpenter, S.N. Laughton, M.R. Wiesner, Enhanced biogas production from nanoscale zero valent iron-amended anaerobic bioreactors, Environ. Eng. Sci. 32 (8) (2015) 647–655, https://doi.org/10.1089/ees.2014.0560.
[114] E. Abdelsalam, M. Samer, Y. Attia, M. Abdel-Hadi, H. Hassan, Y. Badr, Comparison of nanoparticles effects on biogas and methane production from anaerobic digestion of cattle dung slurry, Renew. Energy 87 (2016) 592–598, https://doi.org/10.1016/j.renene.2015.10.053.
[115] H.A. Pyae, W.W. Aye, C. Yossapol, S. Dararatana, Micro-Particle ZVI Inhibition Threshold in Cassava Pulp Bio-Methanation, vol. 12, Environment Asia, 2019, pp. 64–73, https://doi.org/10.14456/ea.2019.64 (Special Issue).
[116] T. Wang, D. Zhang, L. Dai, Y. Chen, X. Dai, Effects of metal nanoparticles on methane production from waste-activated sludge and microorganism community shift in anaerobic granular sludge, Sci. Rep. 6 (1) (2016) 1–10, https://doi.org/10.1038/srep25857.
[117] B. Yu, X. Huang, D. Zhang, Z. Lou, H. Yuan, N. Zhu, Response of sludge fermentation liquid and microbial community to nano zero-valent iron exposure in a mesophilic anaerobic digestion system, RSC Adv. 6 (29) (2016) 24236–24244, https://doi.org/10.1039/C6RA02591A.
[118] T. Jia, Z. Wang, H. Shan, Y. Liu, L. Gong, Effect of nanoscale zero-valent iron on sludge anaerobic digestion, Resour. Conserv. Recycl. 127 (2017) 190–195, https://doi.org/10.1016/j.resconrec.2017.09.007.
[119] R. Eljamal, I. Maamoun, K. Bensaida, G. Yilmaz, Y. Sugihara, O. Eljamal, A novel method to improve methane generation from waste sludge using iron nanoparticles coated with magnesium hydroxide, Renew. Sustain. Energy Rev. 158 (2022), 112192, https://doi.org/10.1016/j.rser.2022.112192.
[120] F.J. Andriamanohiarisoamanana, T. Shirai, T. Yamashiro, S. Yasui, M. Iwasaki, I. Ihara, T. Nishida, S. Tangtaweewipat, K. Umetsu, Valorizing waste iron powder in biogas production: hydrogen sulfide control and process performances, J. Environ. Manag. 208 (2018) 134–141, https://doi.org/10.1016/j.jenvman.2017.12.012.
[121] E. Mutegoa, A. Hilonga, K.N. Njau, Approaches to the mitigation of ammonia inhibition during anaerobic digestion–a review, Water Pract. Technol. 15 (3) (2020) 551–570, https://doi.org/10.2166/wpt.2020.047.
[122] E.N. Richard, A. Hilonga, R.L. Machunda, K.N. Njau, A review on strategies to optimize metabolic stages of anaerobic digestion of municipal solid wastes towards enhanced resources recovery, Sustain. Environ. Res. 29 (1) (2019) 1–13, https://doi.org/10.1186/s42834-019-0037-0.
[123] P. Hlavínek, L. Stříteský, R. Pešoutová, L. Houdková, Biogas production from algal biomass from municipal wastewater treatment, Waste and biomass valorization 7 (4) (2016) 747–752, https://doi.org/10.1007/s12649-016-9488-2.
[124] N. Zhai, T. Zhang, D. Yin, G. Yang, X. Wang, G. Ren, Y. Feng, Effect of initial pH on anaerobic co-digestion of kitchen waste and cow manure, Waste Manag. 38 (2015), https://doi.org/10.1016/j.wasman.2014.12.027, 126-13.
[125] I.S. Budiyono, S. Sumardiono, Kinetic model of biogas yield production from vinasse at various initial pH: comparison between modified Gompertz model and first order kinetic model, Res. J. Appl. Sci. Eng. Technol. 7 (13) (2014) 2798–2805, https://doi.org/10.19026/rjaset.7.602.
[126] F. Raposo, R. Borja, M. Martín, A. Martín, M. De la Rubia, B. Rincón, Influence of inoculum–substrate ratio on the anaerobic digestion of sunflower oil cake in batch

mode: process stability and kinetic evaluation, Chem. Eng. J. 149 (1–3) (2009) 70–77, https://doi.org/10.1016/j.cej.2008.10.001.
[127] G.K. Kafle, S.H. Kim, K.I. Sung, Ensiling of fish industry waste for biogas production: a lab scale evaluation of biochemical methane potential (BMP) and kinetics, Bioresour. Technol. 127 (2013) 326–336, https://doi.org/10.1016/j.biortech.2012.09.032.
[128] S.N. Ugwu, C.C. Enweremadu, Biodegradability and kinetic studies on biomethane production from okra (Abelmoschus esculentus) waste, South Afr. J. Sci. 115 (7–8) (2019) 1–5, https://doi.org/10.17159/sajs.2019/5595.